Resonant patterns in noisy active media

Changsong Zhou and Jürgen Kurths
Institute of Physics, University of Potsdam, PF 601553, 14415 Potsdam, Germany
(Received 14 August 2003; revised manuscript received 11 March 2004; published 18 May 2004)

We investigate noise-controlled resonant response of active media to weak periodic forcing, both in excitable and oscillatory regimes. In the excitable regime, we find that noise-induced irregular wave structures can be reorganized into frequency-locked resonant patterns by weak signals with suitable frequencies. The resonance occurs due to a matching condition between the signal frequency and the noise-induced inherent time scale of the media. $m:1$ resonant regions similar to the Arnold tongues in frequency locking of self-sustained oscillatory media are observed. In the self-sustained oscillatory regime, noise also controls the oscillation frequency and reshapes significantly the Arnold tongues. The combination of noise and weak signal thus could provide an efficient tool to manipulate active extended systems in experiments.

DOI: 10.1103/PhysRevE.69.056210 PACS number(s): 05.40.−a, 05.45.−a, 87.10.+e

I. INTRODUCTION

Pattern formation in spatially extended systems subject to external forcing has been studied extensively [1–9]. In resonantly forced oscillatory reaction-diffusion systems, $m:1$ frequency locking occurs similar to that in a single, uncoupled oscillator. The entrained system has m stable states with phases separated by multiples of $2\pi/m$, i.e., the m-phase patterns, such that traveling waves are stabilized to various standing wave patterns. Such resonant patterns have been observed in light-sensitive Belousov-Zhabotinsky (BZ) reactions under periodic illumination [5].

Periodic illumination has also been applied to control spatially stationary Turing structure. Most efficient suppression of pattern occurs at a frequency of illumination equal to the frequency of autonomous oscillations in a corresponding well-stirred system [6]. Besides temporal (spatially uniform) illuminations, spatial (steady) [7] and spatiotemporal [8] modulations have also been used to study resonant response of Turing patterns. Periodic illumination of spiral waves in excitable BZ reaction can induce entrained drift of the spiral core [9]. Periodically vibrated granular layer can display a rich variety of patterns [10]. Thus, external forcing provides an alternative powerful tool to probe the inherent mechanism and to control the behavior of pattern formation in extended systems, in parallel with global [11] or spatiotemporal [12] feedbacks.

Imperfections and noise are inevitably present in real systems. Complicated front dynamics have been observed in resonantly forced reaction-diffusion systems with spatial or spatiotemporal random forcing amplitudes [13], e.g., due to inhomogeneities in illumination. To our knowledge, effects of noise on resonant pattern formation of self-sustained oscillatory extended systems have not yet been studied. Intuitively noise will have degrading influences based on the knowledge that it usually spoils phase locking of single oscillators by phase slips [14].

On the other hand, the influence of noise on extended systems can actually enhance the pattern-formation mechanism [15]. Such constructive effects include noise-induced transitions [15], noise-enhanced signal propagation in bistable or monostable media [16], noise-sustained wave propagation in subexcitable chemical reactions [17], and spatiotemporal stochastic resonance [18]. In particular, in active media, noise alone can sustain spiral waves [19], target waves [20,21] or pulsating waves [21], and enhances spatial synchronization [22] and temporal coherence [23]. In these systems, the interplay between noise-induced excitation and wave propagation has generated oscillatory behavior with some characteristic time or length scales. However, not much is known how the noise-sustained oscillatory behavior responds to weak external forcing. Recently, we have shown that, unlike in an isolated Fitz Hugh-Nagumo (FHN) excitable cell, in a small one-dimensional (1D) chain of coupled FHN cells, noise-sustained oscillations may become locked by rather weak periodic signals, because coupling enhances significantly the coherence of the noise-sustained oscillations [24].

In this paper we study effects of noise on resonant pattern formation of 2D FHN media forced by spatially uniform, weak periodic signals, both in the excitable and in the oscillatory regimes. We will show that in the excitable regime, due to the influence of noise, signals much weaker than the threshold can induce coherent resonant patterns. In the self-sustained oscillatory regime, instead of simply spoiling locking as intuitively expected, noise controls the natural frequency of the oscillation, and reshapes significantly the locking tongues of the media.

II. EXCITABLE REGIME

Our results are based on numerical simulations of 2D lattices of $N\times N$ ($N=100$) locally coupled Fitz Hugh-Nagumo (FHN) model [22,23], which are paradigmatic for active dynamics in biology or chemical reactions:

$$\epsilon\dot{x}_{ij} = x_{ij} - \frac{x_{ij}^3}{3} - y_{ij} + A\cos\Omega t + \frac{g}{4}\sum_{kl}(x_{kl} - x_{ij}),$$

$$\dot{y}_{ij} = x_{ij} + a + \sqrt{2D}\xi_{ij}(t) \qquad (1)$$

with a periodic boundary condition. Here $(k,l)=(i\pm1, j\pm1)$. With $\epsilon=0.01$ and $a>1.0$, the homogeneous medium is ex-

citable. After a subcritical Hopf bifurcation at $a=1.0$, the system moves into the self-sustained oscillatory regime for $a<1.0$. In this section, we fix $a=1.05$ in the excitable regime. g is the coupling strength and D is the intensity of Gaussian noise $\xi_{ij}(t)$, white in space and time. The lattice is driven uniformly by a periodic signal with a frequency Ω and an amplitude A. This discrete lattice is suitable for the description of excitable biological tissue (e.g., neurons, cardiac cells) [25], and can also be regarded as an approximation of continuum active media (e.g., active chemical reactions) [19]. The model is integrated using a Heun algorithm [15] with a small time step $\delta t=0.001$.

Without forcing ($A=0$), firing elements are a source for waves spreading through the lattice at strong enough coupling g. At small intensities D noise induces clear target waves when random spontaneous nucleations of excitations are rare. At larger D, when g is also relatively large, spreading waves initiated at many random positions may be quick enough to merge and cover almost the whole domain. Afterwards the media achieve a synchronized relaxation back to the vicinity of the homogeneous steady state where another round of noise-induced nucleation starts to sustain pulsating waves (nearly global oscillations) in the media [21,22]. At weaker coupling strength g, e.g., $g=0.03$ considered in this paper, the collision of the waves initiated from many random positions results in rather irregular patterns [Fig. 1(a)]. The spiking sequences of individual cells are erratic [Fig. 1(b)], and the domain does not show a coherent collective oscillation, as seen by almost vanishing fluctuation of the spatial mean value $\langle x\rangle$ over the whole domain [Fig. 1(c)]. Such an irregular regime is quite different from the coherent regime studied previously in 1D chains of coupled FHN cells [24] where strong enough coupling and noise together already induce synchronized oscillations of the chains. However, the interplay of noise excitation and wave propagation has already generated some internal order in the system: the distribution $P(T)$ of the interspike interval T of the cells exhibits a sharp peak at T_p, followed by a broad tail [Fig. 1(d)]. While the long tail related to the stochastic waiting time of noise excitation of the cells is very similar to isolated cells, the

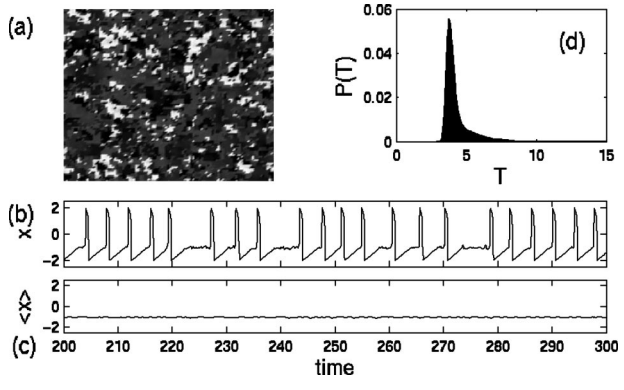

FIG. 1. Typical noise-induced behavior in the media at $g=0.03$ ($D=3\times10^{-4}$). (a) A snapshot of irregular wave patterns, (b) a spike sequence of an element in the lattice, (c) time series of the spatial mean value $\langle x\rangle$, (d) distribution of the interspike interval T of the elements.

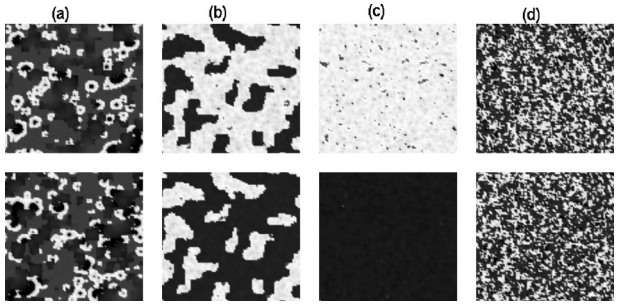

FIG. 2. Patterns at t_1 (upper) and t_1+T_s (bottom) in the presence of subthreshold signal ($A=0.012, \Omega=3.2$) at various noise intensities: $D=0.2\times10^{-4}$ (a), $D=1.0\times10^{-4}$ (b), $D=3.0\times10^{-4}$ (c), and $D=8.0\times10^{-4}$ (d). The moment t_1 corresponds to a local maximum of $\langle x\rangle$ after a transient, and $T_s=2\pi/\Omega$ is the signal period.

sharp peak is mainly a result of propagating waves from the excitation centers in the surrounding area. The peak value T_p is thus controlled by both the coupling strength g and the noise intensity D. The wave patterns and the shape of $P(T)$ are similar for a broad range of noise intensity $5\times10^{-5}\lesssim D\lesssim1\times10^{-2}$. Now we have two time scales in the system: the characteristic firing frequency (CFF) $\Omega_p=2\pi/T_p$ and the mean firing frequency (MFF) $\Omega_a=2\pi/T_a<\Omega_p$ ($T_a=\langle T\rangle_t$ is the time average of T), which are not well expressed in $\langle x\rangle$. Variation of these frequencies vs the noise intensity D for $g=0.03$ is shown later [Fig. 4]. With increasing D, spontaneous nucleation becomes more frequent and denser, so that both the CFF Ω_p and the MFF Ω_a increase, but for small g they are clearly different from each other. There are regions of larger g and corresponding D where the long tail in $P(T)$ is eliminated so that $\Omega_a\approx\Omega_p$; the spiking sequences attain a much higher coherence compared to the most coherent firing behavior in an isolated element [28], a phenomenon called array-enhanced coherence resonance (AECR) [23]. Our recent work [24] in this coherent regime demonstrated that ACER enhances locking of 1D chains to weak signals.

In the following, the media ($g=0.03$) are exposed to both signal and noise, starting from the homogeneous steady state. Reorganization of the patterns in the presence of a subthreshold signal ($\Omega=3.2$, $A=0.012<A_{th}=0.02$, the signal threshold of noise-free media) is shown in Fig. 2. At a rather weak

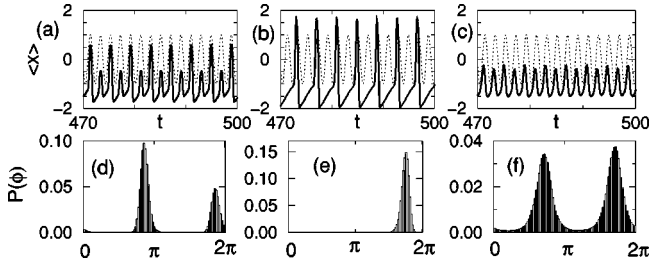

FIG. 3. Time series of the mean field $\langle x\rangle$ (a,b,c) and distribution of spiking phases of all the cells over a long period of time (d,e,f) in the forced media generating different patterns: (a,d) LSW ($D=1.0\times10^{-4}$), (b,e) LPW ($D=3.0\times10^{-4}$) and (d,f) unlocked patterns ($D=8.0\times10^{-4}$). The dotted lines in (a,b,c) indicate the forcing signal.

intensity, e.g., $D=0.2\times10^{-4}$, noise alone can hardly initiate target waves. Together with the weak signal, noise now excites simultaneous many target waves which however, have not been locked by the signal [Fig. 2(a)]. At a larger intensity $D=1.0\times10^{-4}$, the MFF ω of all the cells is locked to the signal with a ratio 2:1, $\omega=\Omega/2$. The medium reorganizes from patterns similar to Fig. 1(a) into two almost uniform domains [Fig. 2(b)], each locked to the signal but with phases differing by π. Such locked standing-wave patterns (LSW) are similar to those observed in self-sustained oscillatory media subject to resonant forcing [3–5] or global feedback [11]. $\langle x\rangle$ now shows a 1:1 phase locking with the signal [Fig. 3(a)], in the sense that there is a smaller or larger spike in each period of the signal. At the larger intensity $D=3.0\times10^{-4}$, the media remain 2:1 locked with the signal, but the spatial patterns become almost uniform [Fig. 2(c)] such that $\langle x\rangle$ also shows a 2:1 phase locking [Fig. 3(b)]. We call such patterns locked pulsating waves (LPW). At even larger intensities, the locking is lost and the patterns become dense, randomly flushing clusters [Fig. 2(d)]; however, $\langle x\rangle$ displays a clear oscillation with a 1:1 phase locking to the signal [Fig. 3(c)]. The waves die out and the media relax to the homogeneous steady states when noise is ceased in simulations.

Phase locking of these noise-sustained waves in the media, however, is not perfect; the domains in Figs. 2(b) and 2(c) are not fully uniform. The spiking phase $\phi_{ij}=\Omega\tau_{ij}$ mod 2π (τ_{ij} being the firing time of the ijth cell) has a distribution $P(\phi)$ with finite width, indicating fluctuations in the firing time. For LSW, the two domains are associated with two separated peaks with a distance of π in $P(\phi)$ [Fig. 3(d)]; while for LPW, there is only one peak [Fig. 3(e)]. For unlocked media [Fig. 2(d)], there are two linked peaks [Fig. 3(f)], since the firing in the random clusters is locked temporally by the signal either around a phase ϕ_1 or $\phi_2=\phi_1+\pi$, and can slip between them. This induces the 1:1 mean-field oscillations in Fig. 3(c). The peak heights in $P(\phi)$ and the amplitudes of $\langle x\rangle$ become smaller with increasing D outside the locking region.

The mechanism underlying frequency locking and resonant pattern formation is a matching of time scales: one time scale is the signal frequency and the other is the noise-induced intrinsic CFF Ω_p. As shown in Fig. 4(a), the frequency locking ($\omega-\Omega/2=0$) is achieved in a range of D around this matching point ($\Omega_p-\Omega/2=0$, $D=1.8\times10^{-4}$), but not around ($\Omega_a-\Omega/2=0$, $D=3.2\times10^{-3}$) where noise-induced MFF matches the signal frequency. In the parameter space of the noise intensity and signal amplitude (D,A), there is a locking region [Fig. 4(b)] similar to the Arnold tongue in self-sustained oscillatory media in the sense that D controls the initial frequency mismatches. Patterns associated to different D and A are indicated by different symbols in Fig. 4(b). Frequency locking and resonant pattern formation occur already for signal amplitudes much smaller than the threshold. When locking is achieved, the fluctuations of the firing time of the cells are reduced significantly by the weak signal. This enhances coherence as measured by $R=\langle T\rangle_t/\sqrt{var(T)}$, which exhibits a clear resonant feature against D for subthreshold signals, and is much higher than R of unforced media [Fig. 4(c), dotted line]. Here the small

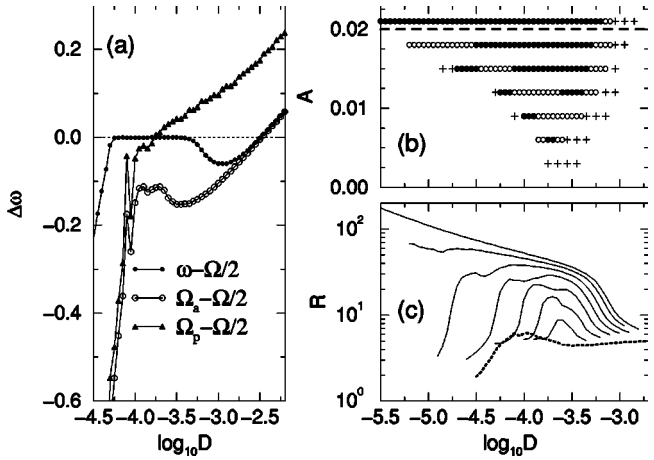

FIG. 4. 2:1 frequency locking regions at a fixed signal frequency $\Omega=3.2$. (a) $A=0.012$. The frequency difference $\omega-\Omega/2$ in the forced media is compared to the matching between the noise-induced ($A=0$) CFF (Ω_p) or MFF (Ω_a) with the signal. (b) The locking region in the parameter space (D, A). The dashed line indicates threshold $A_{th}=0.02$ above which the signal can induce a 2:1 locked response in the noise-free media. The symbols represent different patterns in the forced media: LSW (◦), LPW (•), and unlocked patterns with clear 1:1 oscillations of $\langle x\rangle$ (+). (c) Coherence measure R corresponding to (b), which increases with A and exhibits a resonance for subthreshold signals. The dotted line shows coherence R of unforced media, i.e., $A=0$.

values of R at $A=0$ show again that the system is different from the regime of AECR in 1D chains considered in our previous publication [24].

To verify the time-scale matching condition for resonance, we fix the noise intensity D ($D=3.0\times10^{-4}$ and $\Omega_p=1.62$) and vary the signal frequency in the range $1.0\leqslant\Omega\leqslant6.0$. Figure 5 depicts clearly the 1:1, 2:1, and 3:1 Arnold tongues for Ω around $m\Omega_p$ [26]. Outside but close to these locked regions, mainly on the lower Ω side, there are unlocked patterns with pronounced 1:1 oscillations of the mean field $\langle x\rangle$ [Fig. 5(a), pluses]. In the 1:1 locking region, the media display LPW which can also be observed in the 2:1 and 3:1 regions (closed circles). In the 2:1 and 3:1 regions, the LSW patterns are observed where the media are reorganized into 2 (3) domains which oscillate with phases differing by $2\pi/2$ ($2\pi/3$) (open circles). In all the m:1 cases, the locking is achieved already for rather weak subthreshold signals. The coherence measure R exhibits resonance feature vs Ω, attaining much larger values when moving into the locking regions. The locking regions move with the noise intensity D which controls the CFF Ω_p, but are no longer confined by the superathreshold locking boundaries in the noise-free homogeneous media [Fig. 5(a), solid lines]. At rather small intensities D which do not generate a CFF Ω_p, the locking regions approach to the superathreshold ones. There the locking does not obey the time-scale matching condition.

The locking and resonance in the excitable media due to the time-scale matching condition as studied here is quite different from usual stochastic resonance and noise-enhanced synchronization [27]. There, noise-sustained oscillations of bistable systems do not establish a natural frequency. While

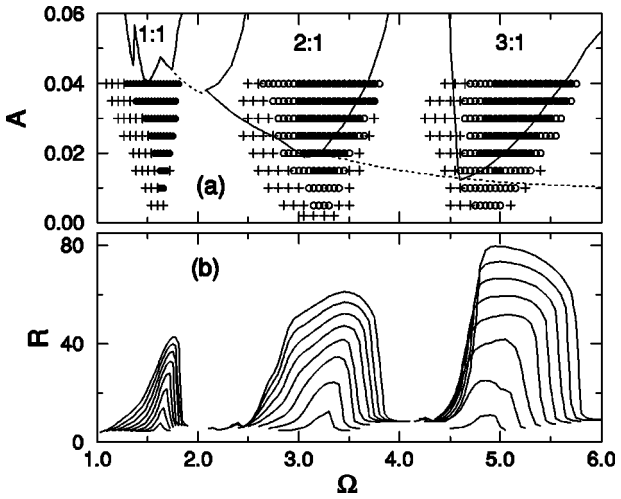

FIG. 5. Response of the media to various signal frequency Ω at fixed noise intensity $D=3.0\times10^{-4}$. (a) 1:1, 2:1, and 3:1 locking regions in the parameter space (Ω,A). The symbols represent different patterns as in Fig. 4(b). The dotted line shows the spiking threshold, and above the solid lines are the superathreshold locking region of homogeneous noise-free media. (b) The corresponding coherence measure R which increases with A.

an effective locking of phase and mean switching frequency is achieved for sufficiently slow signals with amplitudes close to the threshold, it does not obey the time-scale matching condition. The coherence and synchronization measures do not display resonance with respect to the signal frequency Ω [27], and there is no effective high order m:1 $(m>1)$ mean-frequency locking [27].

Besides the similarities, resonant pattern formation of noisy excitable media also bears fundamental difference compared to self-sustained oscillatory media. In the latter case, the local oscillation frequency is close to the autonomous frequency of spatially homogeneous media, with some modulations by diffusive couplings [4]. As a result, the Arnold tongues of the media almost coincide with those of a single oscillator, together with some deviations resulting from these modulations [4,5]. In noisy excitable media, the locking essentially disappears when the cells are decoupled. For homogeneous media subjected to a spatially uniform noise with intensity D (equivalent to a single uncoupled cell), although noise can generate coherent spike sequence due to coherence resonance [28], and coherence measures do show a resonance with the change of both D and Ω [29], we find that the time scale matching does not lead to frequency locking for weak subthreshold signals in the whole range of D. Thus a global noise cannot induce constructive locking behavior in this type of excitable media. This is consistent with previous observations that a global noise cannot induce coherent global oscillations (pulsating waves) of the media [21]. The intrinsic time scale essential for locking by weak signals is necessarily induced by the interplay between the random spontaneous excitations initiated by spatially uncorrelated noise and wave propagation due to coupling. When Ω_p and Ω are close, some part of the media oscillate with its phase locked by the signal. Waves propagating from these locked regions adjust the spiking phase of the neighboring

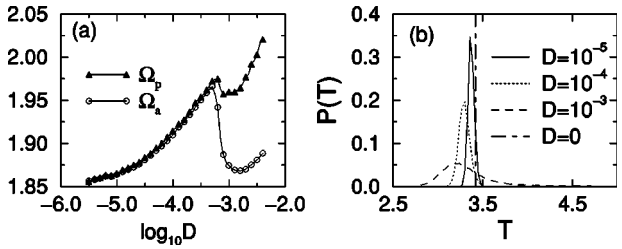

FIG. 6. Effects of noise on controlling the frequency of the self-sustained oscillation $(a=0.99)$. (a) CFF (Ω_p) and MFF (Ω_a) as a function of the noise intensity D. (b) Distribution of the oscillation period T of the oscillators for various noise intensities. The vertical dot-dashed line represents the period of the noise-free oscillator.

regions to entrain a larger domain, so that after a transient the whole media become locked with almost stationary fronts.

Very weak coupling strength g does not support wave propagation in the discrete lattices, and the locking is lost as in decoupled cells. For larger g being able to support pulsating waves of unforced media, the long tail in $P(T)$ is eliminated so that $\Omega_a\approx\Omega_p$; the spiking sequences attain a much higher degree of coherence [23] compared to decoupled cells [28]. In this case, locking of the media can be achieved with almost vanishing signal amplitude $A\sim0$ when $n\Omega=m\Omega_p$ [24], and the resonant patterns are dominantly LPW. While at rather large g, waves propagate very fast to achieve almost perfect global synchronization of the whole domain and the temporal coherence is reduced significantly [23]. The media again act similarly to an isolated cell without a clear frequency locking for subthreshold signals.

III. OSCILLATORY REGIME

Now we consider the self-sustained oscillatory regime by taking the bifurcation parameter $a=0.99$ in Eq. (1), while keeping the coupling strength $g=0.03$ as in the excitable regime. Previous works [1–5] have demonstrated interesting resonant pattern formation in various self-sustained oscillatory media, and here we focus on the effects of noise.

Unlike harmonic self-sustained oscillations for $\epsilon\sim1$ in Eq. (1), with slow-fast variables at $\epsilon\ll1$ in the FHN model and many other active oscillatory models, the rotation along the periodic orbit is rather nonuniform. The trajectory passes by the unstable fixed point rather closely where it slows down, resulting in relaxation oscillations. In the presence of a small noise, the system is rather sensitive to perturbation only when it is in the vicinity of the fixed point where noise becomes dominant and kicks the trajectory to escape earlier on average. While this only influences slightly the geometry of the orbit, it can alter the oscillation frequency clearly as depicted in Fig. 6. For small noise, wave propagation survives, but the oscillation period T starts to fluctuate; the distribution $P(T)$ of T becomes broader and the peak shifts to smaller values with increasing noise level [Fig. 6(b), $D=0$, $D=10^{-5}$ and $D=10^{-4}$]. Accordingly, CFF Ω_p and MFF Ω_a, which are almost the same in this region, increase with D [Fig. 6(a)]. At a threshold noise level $D\simeq5.0\times10^{-4}$, the

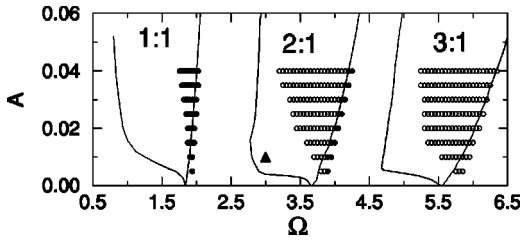

FIG. 7. Locking regions of the oscillatory media ($a=0.99$) at the noise intensity $D=3.0\times10^{-4}$. The symbols represent different patterns as in Fig. 4(b). The Arnold tongues of the noise-free homogeneous media are shown by the solid lines for a comparison. The filled triangle in the 2:1 locking region corresponds to the results in Fig. 8.

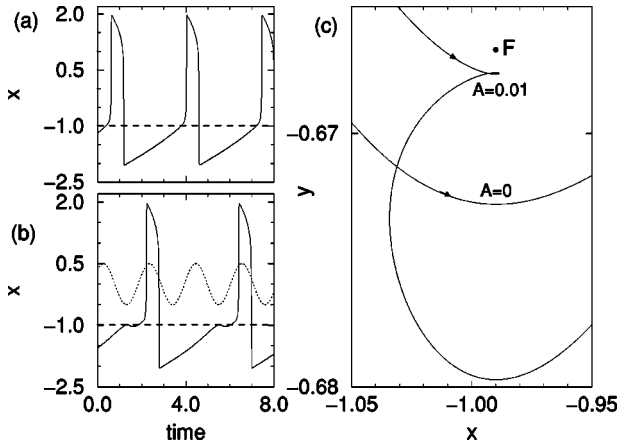

FIG. 8. Comparison of the orbit of an autonomous oscillator ($A=0$) (a) with the orbit of a forced oscillator ($\Omega=3.0$, $A=0.01$) (b). The dashed lines in (a) and (b) show x value at the unstable fixed point, $x_F=-0.99$, and the dotted line in (b) indicates the periodic forcing. (c) The corresponding orbits in the phase space (x,y), in a close vicinity of the unstable fixed point F.

waves fail to survive. After the transition the noisy pattern becomes irregular similar to that in Fig. 1(a). $P(T)$ now is quite broad and asymmetric, with a long tail at large T [Fig. 6(b), $D=10^{-3}$]. The MFF Ω_a drops abruptly and is clearly smaller than CFF Ω_p due to the long tail in $P(T)$, as is similar to the case in the excitable regime [see Fig. 4(a)]. Such a transition at the critical noise level seems to be related to directed percolation [30], however, a detailed analysis is out of the scope of the present work.

The two effects induced by noise, i.e., fluctuation of spiking periods T which on average shift to smaller values, have significant impact on the response of the media to weak signals. In Fig. 7, we compare the Arnold locking tongues of the media at noise intensity $D=3.0\times10^{-4}$ to the tongues of the noise-free media. In the noise-free media, the tips of the locking region are located at multiples of the natural frequency $m\Omega_p$ as a result of time scale matching. The locking regions are quite asymmetrical for a stronger signal amplitude A, extending to signal frequencies Ω much smaller than $m\Omega_p$. To understand the asymmetry of the locking regions, we compare the trajectory of an oscillator in the autonomous medium to that in the locking region ($\Omega=3.0$, $A=0.01$, indicated by the filled triangle in the 2:1 locking region in Fig. 7). It is seen that the forced oscillator [Fig. 8(b)] slows down to perform some small oscillations around the fixed point $x_F=-0.99$; such small oscillations are not present in the autonomous oscillator in Fig. 8(a). Figure 8(c) depicts the corresponding orbits in a close vicinity of the unstable fixed point F in the phase space (x,y). These plots show that slow signals with appropriate amplitudes may lock the oscillations when the orbit is pushed closer to the fixed point F and stays in the neighborhood of F for a longer time to match the period of the signal. Note that the orbits away from F are kept almost unchanged by the forcing signal. The behavior is similar for other values of (Ω,A) in the asymmetrical locking regions, but the detailed oscillation patterns close to F are different. In the presence of noise, the trajectory can no longer perform those tiny oscillations very close to F as in the noise-free media. The locking tongues thus become much more symmetrical. The tips of the locking regions shift to a larger frequency, now at the noise-controlled CFF $m\Omega_p$. As a combined result of the noise effects, the locking regions have been reshaped significantly, which is of importance for resonant pattern formation in experimental systems where noise is inevitably present.

So far the results presented in the excitable regime and in the oscillatory regime are obtained with a spatially uniform initial condition. We have checked that the frequency locking behavior is the same for random initial conditions and for different realizations of noise. The detailed resonant pattern, however, depends on the initial conditions and the realizations of noise.

IV. DISCUSSION

Two fields of investigation of spatially extended systems, resonant pattern formation in periodically forced self-sustained oscillatory media and noise-sustained pattern formation in excitable media, have received a great deal of recent interest. Our work in this paper is on the borderline of these two fields. On the one hand, we have studied effects of periodic forcing on noise-sustained wave structures in the excitable regimes. On the other hand, we have considered effects of noise on resonantly forced self-sustained oscillatory media. In both regimes, we have demonstrated interesting resonant pattern formation and phase locking behavior. In the excitable regime, a weak subthreshold signal can be used to probe noise-induced internal order (here the CFF Ω_p) of the media and to control the originally irregular wave structures into coherent resonant waves patterns. The resonance and frequency locking occur when the signal frequency is close to a rational ratio $(m:n)$ of the noise-induced CFF of the media. The locking and resonance should be observed also in subexcitable media where multiplicative noise induces transitions to excitable or oscillatory regime and initiates waves. Noise also affects the dynamics in the oscillatory regime. The resonant response regions to weak signal have been reshaped significantly. The results suggest that noise, when combined with an weak signal, could be a very useful tool to manipulate active extended systems, such as the excitable [20] or subexcitable [17] BZ reactions in

experiments or natural systems such as the cardiac tissue [25].

Active excitable or oscillatory dynamics in spatially extended systems, together with noise, are very relevant to calcium signaling in living cells. Spatiotemporal patterns and waves of calcium signals have been observed experimentally [31]. Recent theoretical analysis has demonstrated the importance of stochastic release kinetics for calcium waves [30,32]. In particular, noise-sustained oscillation and AECR have been observed in a stochastic fire-diffusion-fire model of calcium release [33]. Our results in this paper suggest that such noise-sustained oscillations may be entrained by a weak signal, which could be meaningful for regulation of calcium signaling.

Noise enhanced internal coherence has also been observed in vivo cat spinocortical nerve systems [34]. Our results on locking and resonance may provide an explanation for noise-induced entrainment in human brain waves [35] which are manifestation of collective oscillations in coupled excitable neurons subject to internal synaptic noises and external noises. Thus the control of wave structure and collective behavior by noise and weak signals may have a wealth of potential implications for active chemical, biochemical, cardiology and neurophysiology systems. In the biological context, the couplings are usually not regular. The influences of network topology on the resonant response are under investigation.

ACKNOWLEDGMENTS

The authors thank R. Steuer for helpful discussions. This work was supported by the Humboldt Foundation (C.Z.) and SFB 555 (D.F.G.).

[1] H. Riecke, J. D. Crawford, and E. Knobloch, Phys. Rev. Lett. **61**, 1942 (1988); I. Rehberg *et al.*, *ibid.* **61**, 2449 (1988).
[2] P. Coullet and K. Emilsson, Physica D **61**, 119 (1992); H. Chaté, A. Pikovsky, and O. Rudzik, *ibid.* **131**, 17 (1999).
[3] C. Elphick, A. Hagberg, and E. Meron, Phys. Rev. Lett. **80**, 5007 (1998); Phys. Rev. E **59**, 5285 (1999); A. L. Lin *et al.*, *ibid.* **62**, 3790 (2000); R. Gallego *et al.*, *ibid.* **64**, 056218 (2001).
[4] H. K. Park, Phys. Rev. Lett. **86**, 1130 (2001).
[5] V. Petrov, Q. Ouyang, and H. L. Swinney, Nature (London) **388**, 655 (1997); A. L. Lin *et al.*, Phys. Rev. Lett. **84**, 4240 (2000).
[6] A. K. Horváth *et al.*, Phys. Rev. Lett. **83**, 2950 (1999); M. Dolnik, A. M. Zhabotinsky, and I. R. Epstein, Phys. Rev. E **63**, 026101 (2001).
[7] M. Dolnik *et al.*, Phys. Rev. Lett. **87**, 238301 (2001).
[8] S. Rüdiger *et al.*, Phys. Rev. Lett. **90**, 128301 (2003).
[9] O. Steinbock, V. Zykov, and S. Müller, Nature (London) **366**, 322 (1993).
[10] F. Melo, P. Umbanhowar, and H. L. Swinney, Phys. Rev. Lett. **72**, 172 (1994); **75**, 3838 (1995); P. Umbanhowar, F. Melo, and H. L. Swinney, Nature (London) **382**, 793 (1996).
[11] V. K. Vanag *et al.*, Nature (London) **406**, 389 (2000); M. Kim *et al.*, Science **292**, 1357 (2001).
[12] T. Sakurai *et al.*, Science **296**, 2009 (2002); C. K. Tung and C. K. Chan, Phys. Rev. Lett. **89**, 248302 (2002); O. Beck *et al.*, Phys. Rev. E **66**, 016213 (2002).
[13] C. J. Hemming and R. Kapral, Chaos **10**, 720 (2000).
[14] R. L. Stratonovich, *Topics in the Theory of Random Noise* (Gordon and Breach, New York, 1963).
[15] J. Garcia-Ojalvo and J. M. Sancho, *Noise in Spatially Extended Systems* (Springer, New York, 1999).
[16] M. Löcher, D. Cigna, and E. R. Hunt, Phys. Rev. Lett. **80**, 5212 (1998); J. F. Lindner *et al.*, *ibid.* **81**, 5048 (1998); A. A. Zaikin *et al.*, *ibid.* **88**, 010601 (2002).
[17] S. Kádár *et al.*, Nature (London) **391**, 770 (1998); L. Q. Zhou *et al.*, Phys. Rev. Lett. **88**, 138301 (2002).
[18] P. Jung and G. Mayer-Kress, Phys. Rev. Lett. **74**, 2130 (1995); J. F. Lindner *et al.*, *ibid.* **75**, 3 (1995); F. Marchesoni *et al.*, *ibid.* **76**, 2609 (1996); J. M. G. Vilar and J. M. Rubí, *ibid.* **78**, 2886 (1997).
[19] J. Garcia-Ojalvo and L. Schimansky-Geier, Europhys. Lett. **47**, 298 (1999); Z. Hou and H. Xin, Phys. Rev. Lett. **89**, 280601 (2002).
[20] S. Alonso *et al.*, Phys. Rev. Lett. **87**, 078302 (2001); S. Alonso, F. Sagués, and J. M. Sancho, Phys. Rev. E **65**, 066107 (2002).
[21] H. Hempel *et al.*, Phys. Rev. Lett. **82**, 3713 (1999).
[22] A. Neiman *et al.*, Phys. Rev. Lett. **83**, 4896 (1999).
[23] B. Hu and C. S. Zhou, Phys. Rev. E **61**, R1001 (2000); C. S. Zhou, J. Kurths, and B. Hu, Phys. Rev. Lett. **87**, 098101 (2001).
[24] C. S. Zhou, J. Kurths, and B. Hu, Phys. Rev. E **67**, 030101(R) (2003).
[25] J. M. Davidenko *et al.*, Nature (London) **355**, 349 (1992).
[26] A relatively smaller 1:2 locking region around $\Omega=\Omega_p/2$ also shows up at larger signal amplitudes, where the threshold A_{th} is also much larger.
[27] A. Neiman *et al.*, Phys. Rev. E **58**, 7118 (1998); J. A. Freund, A. Neiman, and L. Schimansky-Geier, Europhys. Lett. **50**, 8 (2000).
[28] G. Hu *et al.*, Phys. Rev. Lett. **71**, 807 (1993); A. S. Pikovsky and J. Kurths, *ibid.* **78**, 775 (1997).
[29] A. Longtin and D. Chialvo, Phys. Rev. Lett. **81**, 4012 (1998); B. Lindner and L. Schimansky-Geier, Phys. Rev. E **61**, 6103 (2000).
[30] M. Bär *et al.*, Phys. Rev. Lett. **84**, 5664 (2000).
[31] *Calcium Signalling (Methods in Signal Transduction)*, edited by J. W. Putney (CRC Press, London, 1999).
[32] M. Falcke, L. Tsimring, and H. Levine, Phys. Rev. E **62**, 2636 (2000).
[33] S. Coombes and Y. Timofeeva, Phys. Rev. E **68**, 021915 (2003).
[34] E. Manjarrez *et al.*, Neurosci. Lett. **326**, 93 (2002).
[35] T. Mori and S. Kai, Phys. Rev. Lett. **88**, 218101 (2002).